Archaeological and Anthropological Sciences (2021) 13: 154
https://doi.org/10.1007/s12520-021-01427-9

ORIGINAL PAPER

The earliest known Italian case of bilateral non-osseous calcaneonavicular coalition from the mediaeval cemetery of Troina (Enna, Sicily)

Elena Varotto[1,2] · Lorenzo Zurla[3] · Francesco M. Galassi[1,2] · Caterina Ingoglia[3]

Received: 29 April 2021 / Accepted: 5 August 2021 / Published online: 23 August 2021

Abstract
In this article, we detail a case of tarsal coalition in the osteological remains of an adult female individual from the mediaeval cemetery of the Catena district of Troina (Enna, Sicily). The burial that contains the skeleton described in this work (*Burial 2*) was subjected to a multidisciplinary analysis starting from the excavation on the field and ending with a full palaeopathological study including palaeoradiology and 3D virtual reconstructions. The obtained results contribute to our understanding of this congenital condition in the past and represent, to the best of our knowledge, the first case ever reported from Sicily and the Italian peninsula of bilateral non-osseous calcaneonavicular tarsal coalition.

Keywords Palaeopathology · Palaeoradiology · Congenital disease · Foot · Tarsal coalition · Middle Ages · Sicily

Introduction

Archaeological contextualisation

The archaeological investigations conducted in Troina (province of Enna, central Sicily, Fig. 1) between the 1950s and 1980s brought to light, in the area of Muanà, the remains of the Hellenistic and Roman necropolis of an ancient settlement whose name is still unknown (Militello 1961; Scibona 1980). A new archaeological research, this time launched by the University of Messina, started in 2017 and is still ongoing. Stratigraphic excavations identified a new cemetery in a state-owned area called *Catena*, immediately south of modern-day Troina. The necropolis extends over a vast area whose limits have not yet been defined. Thirty-six inhumation tombs have been found so far — between 2017 and 2019 — and none of them has been shown to contain grave goods. All of them cover — in some cases lean onto or cut — the remains of potentially public and housing structures archaeologically dated to the Hellenistic and (Late) Roman/Byzantine periods.

The *Catena* area is characterised by a steep slope, hence the formation of the earth layers, which have accumulated after the abandonment of the oldest structures, has been strongly conditioned by important runoff processes. Therefore, the retrieved ceramics, dated to a period between the Hellenistic Age and the seventeenth century AD, appear mixed. It was through the stratigraphic excavation that it finally became possible to establish the relative chronology of the necropolis: the (Late) Roman/Byzantine evidence represents the *terminus post quem*, while a few fragments of 17th-century ceramics are the *terminus ante quem*.

Tarsal coalition: anatomical and pathological aspects

Tarsal coalition as a pathological condition was first scientifically described by Georges-Louis Leclerc de Buffon (1707–1788) in 1769 (Docquier et al. 2019), while the first palaeopathological report in a pre-Columbian Indian specimen was made by Heiple and Lovejoy (1969). Later, the condition was also dated back to as early as 9,300 years ago

Francesco M. Galassi and Caterina Ingoglia shared last authorship.

✉ Elena Varotto
elena.varotto@flinders.edu.au

[1] Archaeology, College of Humanities, Arts and Social Sciences, Flinders University, Adelaide, SA, Australia

[2] FAPAB Research Center, Pz. Umberto I n°5, 96012 Avola (SR), Sicily, Italy

[3] Department of Ancient and Modern Civilizations, University of Messina, Messina, Italy

Fig. 1 Map of Sicily from Google Earth. The red pin indicates the location of Troina (Enna, Sicily). Geographic coordinates: latitude 37°46′53″N–longitude 14°35′55″E; 1,000 m above sea level

in the Kennewick Man (Case 2014) and the Late Neolithic and Chalcolithic periods (Silva 2005).

This condition, mostly congenital, is characterised by a fusion of two or more tarsal bones resulting from a failure in mesenchymal separation during the 8-week-long embryonic development (Case and Burnett 2012). From a genetic perspective, its origin is to be found in described missense mutations in the NOG gene, which can lead to tarsal/carpal coalition syndrome (TCC) (Dixon et al. 2001). However, tarsal coalition can also be acquired, as the result of other conditions such as degenerative joint disease, trauma, inflammatory arthritis, tumour, infection, and clubfoot deformities (Bohne 2001). It can be either osseous or non-osseous, either unilateral or bilateral (Albee 2020). It has an autosomal dominant inheritance pattern and a nearly full penetrance (Leonard 1974). As far as its frequency is concerned, recent studies (Case and Burnett 2012) performed on skeletal collections of European Americans, mediaeval Danes, native South Africans and drawing from data from cadaveric research (Pfitzner 1896; Rühli et al. 2003) have suggested it to be 2–5%. This last percentage is higher than the 1–2% found in clinical studies (Case and Burnett 2012), which may be explained by the fact that not all cases of tarsal coalition ultimately lead to a painful presentation in living patients (Kulik and Clanton 1996) and also by a potential misdiagnosis of this condition in ancient skeletons as degenerative joint disease (DJD) when they are analysed by physical anthropologists (Case and Burnett 2012). Its incidence is unknown but estimated by some to be around 1% (Stormont and Peterson 1983; Kulik and Clanton 1996). Moreover, most studies seem to indicate an equal sex incidence or male predominance (Kulik and Clanton 1996).

All tarsal bones can be involved in this condition. Based on the involved segments, there can be different tarsal coalitions (TCs): calcaneonavicular (CN), talocalcanear (TC), talonavicular, calcaneocuboid, cuneocuboid, cuneometatarsal, calcaneocuboid, cuneometatarsal, cubonavicular, etc. The first two (CN and TC) are the most frequent ones (Silva and Silva 2010) and CN typically ossifies between 8 and 12 years unless it remains non-osseous (Silva 2005).

According to Harris (Harris 1955, 1965), tarsal coalitions can be complete or incomplete: the complete type is fully ossified (*synostosis*), while the incomplete one is not completely ossified with fibrous tissue (*syndesmosis*), cartilage (*synchondrosis*), or a combination of both. However, other authors (Kulik and Clanton 1996) prefer to opt for three types of coalition: ossified coalition composed of bone, non-ossified coalition composed of fibrous, and/or cartilaginous tissue, partially ossified (bone mixed with fibrous/cartilaginous tissue). In addition, non-osseous coalitions leave a recognisable mark on the bones (Albee 2020). This mark varies in presentation depending on the nature of the bridge, whether it be fibrous or cartilaginous (Albee 2020): the former causes a lesser degree of alteration of the bone surface such as subchondral sclerosis or some narrowing of the articular space (Albee 2020), while the latter can also present with cystic lesions which can lead to the exposure of trabeculae (Silva 2011). Sometimes these cystic lesions happen to host nodular bone formations (Hynes and Romash 1987). Clinically, tarsal coalition can be symptomatic or

asymptomatic and associated with other conditions such as peroneal spastic flatfoot, rigid valgus of the hindfoot and forefoot (Kulik and Clanton 1996), gross limb abnormalities (phocomelia, hemimelia, etc., Leonard 1974), Apert's syndrome, arthrogryposis and symphalangism (Aufderheide and Rodríguez-Martín 2011), Muenke syndrome (Agochukwu et al. 2013), and Crouzon syndrome (Craig and Goldberg 1977).

With particular reference to calcaneonavicular coalition, a list of palaeopathological cases is provided in Table 1.

Materials and methods

The excavation was documented through multiple photographic acquisitions generating photogrammetric plans for the two-dimensional data (Jaff 2005), integrated with appropriate topographic surveys of the acquired targets with a total station, i.e. the 'photoplans', made for each cut and used for the planimetric documentation (Fig. 2a–e). Through the same acquisition, the raster data have been processed with stereophotogrammetric elaborations (Fiorini and Archetti 2011) that allow us to document the three-dimensional

Table 1 Known cases of osseous and non-osseous calcaneonavicular coalitions reported in the paleopathological literature according to the year of publication (modify from Case and Burnett 2012)

Site/location	Chronology	Form	Side	Age–sex	Author(s)
France	Early Middle Age (Merovingian Age)	Asymmetrical	Bilateral — bone fusion on the right side, close contact on the left	Adult–unknown	Dastugue and Metz 1977
Lerna, Greece	Middle Bronze Age	Non-osseous (NOC)	Unilateral — left	Adolescent (15 yrs)–male	Angel 1971
Serra da Roupa, Portugal	Late Neolithic/Chalcolithic	Non-osseous (NOC)	Right calcaneum — not recordable if unilateral or bilateral	Adult–unknown	Silva 2005
Hipogeu de Sao Paulo II, Portugal	Late Neolithic/Chalcolithic	Non-osseous (NOC)	Left calcaneum and right navicular — not recordable if unilateral or bilateral	Juvenile (near 18 yrs)–male	Silva 2005
Larina Le Mollard, France	Mediaeval	Non-osseous (NOC)	Bilateral	Adult–unknown sex	Darton 2007
Dorset, England	Late Roman	Non-osseous (NOC)	Unilateral — right	Adult (c. 23–26 yrs)–male	Dinwiddy 2009
Sintra, Portugal	Late Roman (second–fourth centuries AD)	Non-osseous (NOC)	Unilateral — right	Adult–female	Silva and Silva 2010
Odense, Denmark*	Mediaeval	Non-osseous (NOC)	See the footnote*	See the footnote*	Case and Burnett 2012
Almada, Portugal	Late Neolithic	Non-osseous (NOC)	Right navicular — not recordable if unilateral or bilateral	Individual of unknown sex	Silva 2011
Kennewick Man, USA	Early Holocene (ca. 7000 BC)	Non-osseous (NOC)	Bilateral	Adult–male	Case 2014
Prague-Zličín, Czech Republic	Migration Period (fifth century)	Osseous (OSC)	Unilateral — left	Adult (45–50 yrs)–female	Vargová et al. 2016
Exeter, England	From late eighth century until 1636	Non-osseous (NOC)	Unilateral — left	Adult–unknown	Albee 2020
Exeter, England	From late eighth century until 1636	Non-osseous (NOC)	Bilateral	Old middle adult–female	Albee 2020
Exeter, England	From late eighth century until 1636	Non-osseous (NOC)	Unilateral — right	Old middle adult–male	Albee 2020
Exeter, England	From late eighth century until 1636	Non-osseous (NOC)	Unilateral — right	Adult (18 +)–female	Albee 2020
Exeter, England	From late eighth century until 1636	Non-osseous (NOC)	Unilateral — left	Old middle adult–male	Albee 2020
Troina, Italy	Mediaeval (1250–1301 AD)	Non-osseous (NOC)	Bilateral	Adult–female (30-40 yrs)	Varotto et al. 2021, present study

*11 cases of non-osseous calcaneonavicular coalitions (5 males, 6 females: 4 bilateral, 3 unilateral, 4 side not specified)

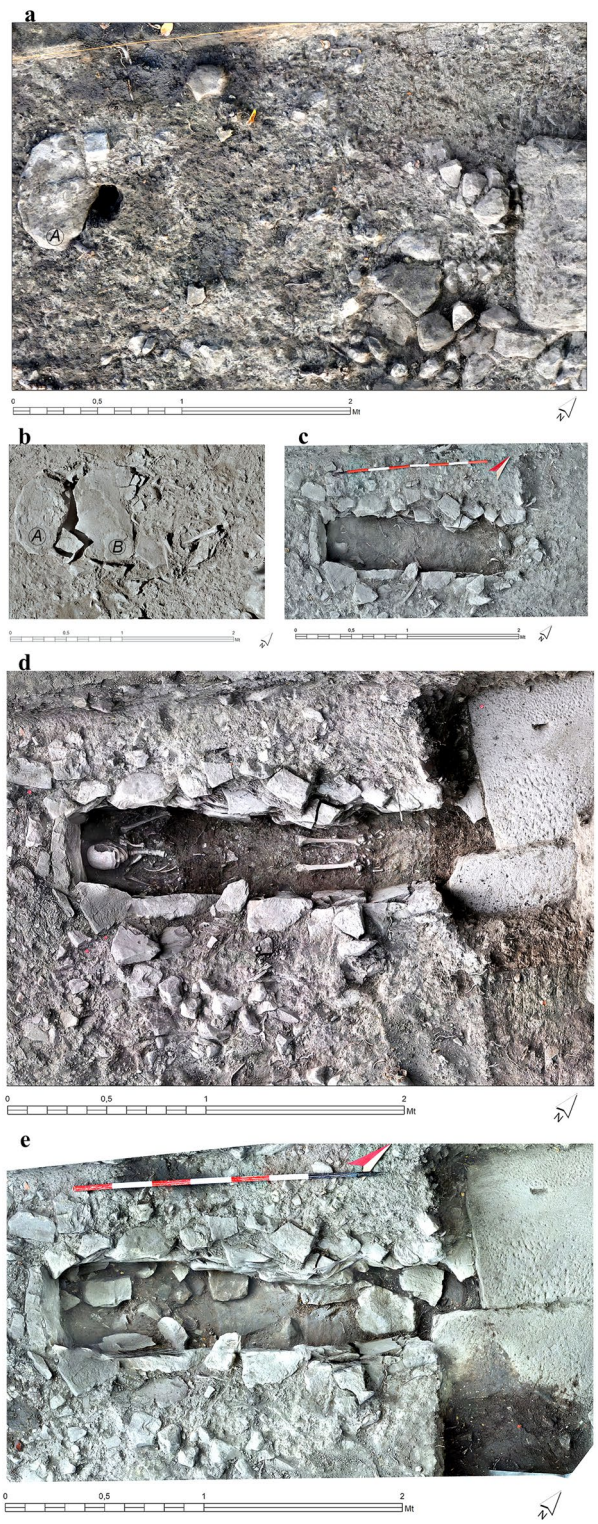

Fig. 2 GIS layout of the excavation levels with photogrammetric basemap of *Burial 2* (**a**–**e**)

stratigraphic (used open source softwares: Meshroom 2017 1.0, https://alicevision.org/ e Blender 2.79, https://www.blender.org/), structural, and anthropometric aspects of the burial (Fig. 3a–c).

The archaeological plans of the interfaces and depositional level were made realised digital drawing with a drawing table, digitising (Photoshop elements 7.0) the evidence on the layouts exported from the GIS platform (Software QGIS 3.14.0, https://qgis.org/en/site/forusers/download.html) of the 'ArcheoTroina' project (Fig. 4).

The retrieved skeleton was subjected to a comprehensive anthropological and palaeopathological analysis, following the workflow adopted for the *Sicily Paleopathology Project* (FAPAB Research Center) (Varotto et al. 2021).

The quantitative state of preservation was calculated using the Bello (2001) indexes: BRI (Bone Representation Index) expressed as the ratio between the number of found bones and the theoretical number of bones that should be present in the actual total palaeodemography obtained from the number of individuals found in anatomical connection; API (Anatomical Preservation Index) expressed as the ratio of conservation scores (in percentage) attributed to each bony element constituting the skeleton and the total number of bones of the skeleton (as defined in Bello 2001).

Sex was determined through the analysis of cranial and pelvic morphologies (Ferembach et al. 1977–1979), while the individual's age at death was estimated based on the changes of the auricular surface of the ilium and the pubic symphysis and on recorded degree of dental wear (Lovejoy et al. 1985; Brooks and Suchey 1990; Lovejoy 1985). The measurements were taken with a digital sliding caliper. Radiocarbon dating was also performed in order to date this skeleton.

Stature was calculated using the Trotter and Gleser formula (Trotter and Gleser 1952; 1977).

For the diagnosis of tarsal coalition, the methodologies proposed by Kulik and Clanton (1996) and by Case and Burnett (2012) were implemented. A palaeoradiological study was performed using X-rays and CT scans (X-ray equipment and parameters: General Medical Merate opera T90 ce; 50 kV 200 mA 160 mS; CT scan equipment and parameters: GE Healthcare Medical System Brightspeed; 120 kV 160 mA 35 mAs, slice thickness: 1.25 mm). 3D virtual reconstruction of the tarsal coalitions was made using OsiriX (v. 11.0.4).

Results

The skeleton was found inhumated in a primary single burial built with roughly carved stones and lithic slabs, which surrounded and covered the deceased (Fig. 2a, b). The burial has a maximum length of 189 cm, an average width of

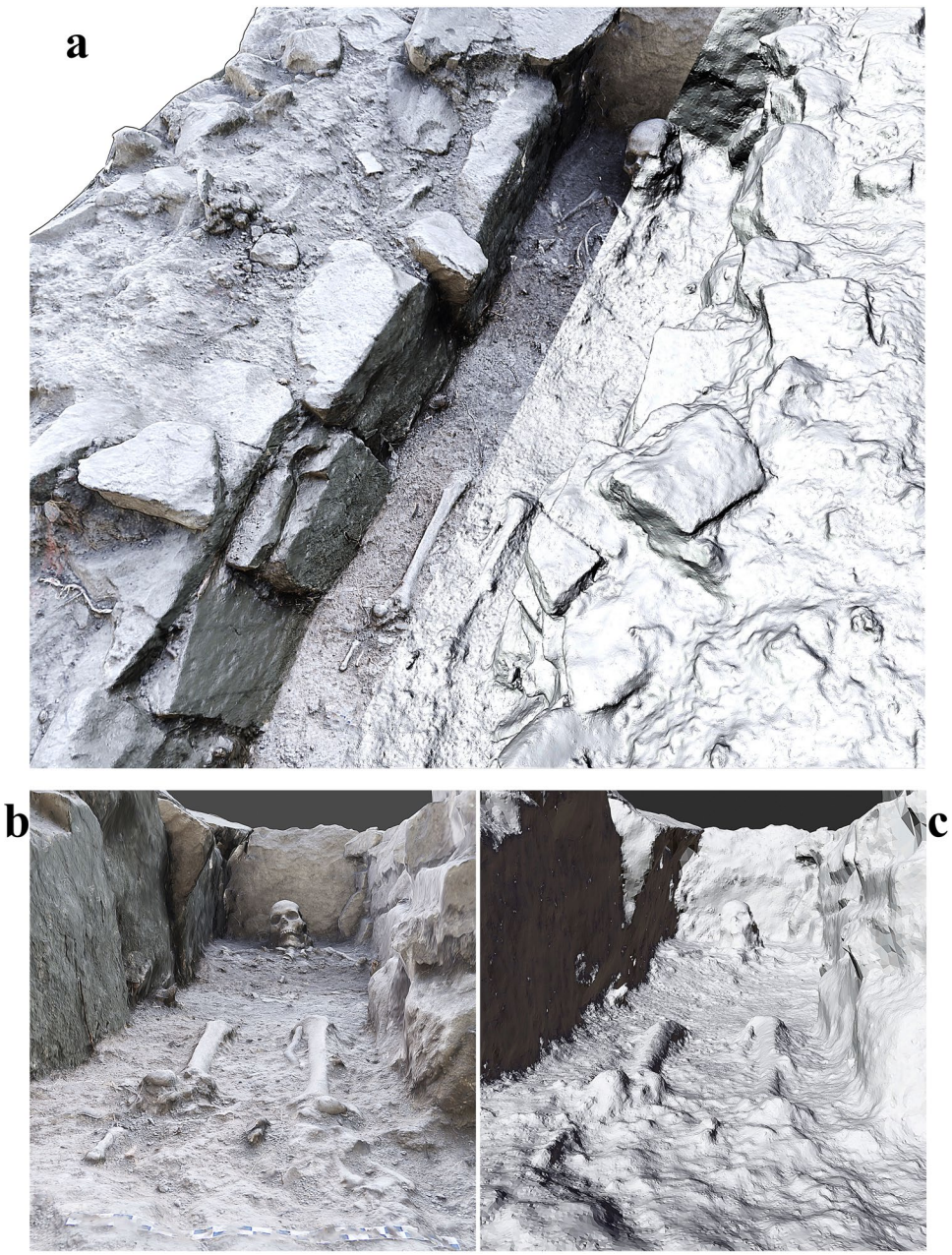

Fig. 3. 3D model from stereo-photogrammetric elaborations. Oblique view from North-West (**a**) and view from inside the burial (**b**–**c**)

45 cm, and a maximum depth of 61 cm (Fig. 2c). Its cover was identified 37 cm under the current ground level. According to established archaeological stratigraphic principles (Carandini 2010), a horizontal excavation was performed using light tools for artificial cuts of approximately 10 cm: the ground filling of the grave that contained the skeleton belonged to one single stratigraphic unit (Fig. 2d). The burial had not been violated in the past but had been heavily disturbed by the large roots of a nearby tree. They had penetrated the burial from the west side and between slabs A and B (Fig. 2b) causing the collapse of part of the perimeter structure as well as three covering slabs. The roots heavily altered the anatomical disposition of the bones, especially of the thoracic and lumbar vertebrae, pelvis (including sacrum), and femora. Following the removal of the osteological remains, a funerary bed composed of natural lithic slabs and medium-sized stones was found. Additionally, between the deceased's shoulder regions, two stones had been parallelly located with the aim of supporting the skull in its correct anatomical position (Fig. 2e).

The skeleton was found almost complete and its state of preservation was good: $BRI = 62.71\% =$ class 4; $API = 85.06\% =$ class 5 (Fig. 5). The individual was anthropologically determined to be an adult female with a mean age at death of 35 years (range: 30-40 yrs). Stature was calculated from the length of the left humerus yielding

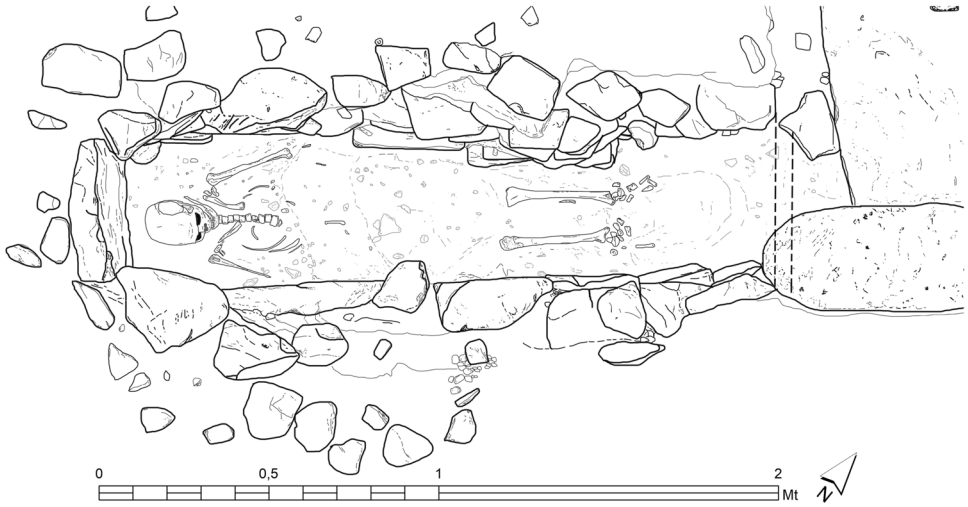

Fig. 4 Planimetry of the depositional level of *Burial 2*

149.7 cm (SD ± 4.45) and from that of the left femur yielding 151.4 cm SD + − 3.72, with an average of 150.5 cm. The skeleton was radiocarbon dated to AD 1250–1301 (1σ).

The structure of both calcanei and navicular bones shows an abnormal morphological presentation: the anterior talar articular facet of both calcanei appears almost disappeared and presents substantial pitting, cystic formations with the exposure of internal trabecular bone within well-defined margins (Fig. 6b–d); the facets also form an abnormally oblique angle between the calcanei and navicular bones. In addition, the navicular bones have a matching lesion with a comparable morphology (pits, cystic lesions, roughened surface) are larger than normal in size and they also include part of the articular facet for the cuboid bone of the calcanei on their plantar aspect (Figs. 6a and 7a–c).

Regarding the measurements, the length of the right calcaneus is 76.8 mm, the length of the left calcaneus is not recordable because the posterior part is broken. The area of the lesion in the right calcaneus has a long axis of 23 mm and a mean width of 4.2 mm, while in the left calcaneus it has a long axis of 25.6 mm and a mean width of 8.4 mm. A matching lesion was found on both navicular bones. The length of the right navicular bone is 35.4 mm, while that of the left navicular bone is 35 mm. The lesion in the right navicular bone has a long axis of 23.5 mm and a mean width of 6.4 mm, while in the left navicular bone, the long axis of the lesion is 25.1 mm and the mean width is 10.8 mm.

These typical features observed on the external morphology on the foot bones can also be better appreciated through radiological (X-ray and CT scan) images (Fig. 8a–c). To the best of our knowledge, this should be the first time an ancient case of calcaneonavicular tarsal coalition has been subjected to a CT scan analysis: interestingly, a circular lack of bone tissue surrounded by a radiopaque dense sclerotic bone was found in the navicular bones precisely in the point where there is the failed segmentation (Fig. 8c). For a modern example of this radiological finding, see https://radiopaedia.org/play/6328/entry/91505/case/7597/studies/8422?lang=us.

Moreover, on a sagittal CT scan view of the right and left calcanei, a tubular prolongation is present: this particular structure extends anteriorly of the superior part of the calcaneus, a conformation which resembles the nose of an anteater (Fig. 9), after which this radiological sign is named 'anteater nose sign' (Oestreich et al. 1987). A 3D virtual reconstruction from CT scans is also provided (Fig. 10).

Discussion

By comparing the collected data with the published palaeopathological and clinical literature, this case fits the main morphological and radiological criteria (Case and Burnett 2012): matching lesion between the calcanear and navicular bones with cystic, roughened, pitted appearance of the tissue and exposure of trabeculae surrounded by well-defined walls; absence of the anterior talar facet; facet for cuboid on navicular bone; oblique angle formed between the calcaneus and navicular; presence of 'anteater nose sign'. Specifically, the radiologically described evidence of the 'anteater nose sign' (Fig. 9) directly suggests a diagnosis of calcaneonavicular tarsal coalition (Oestreich et al. 1987), even though it is not always present in all cases of this condition. To this, the presence of bilateral abnormal sloping of *sustentaculum tali* (Fig. 8b) can be added as further evidence.

All these features together lead us to the diagnosis of bilateral non-osseous calcaneonavicular coalition. Despite the expected limitation imposed by the dry specimen, we maintain that this case can be classified as of the cartilaginous type on account of the pitting appearance of the articular facets.

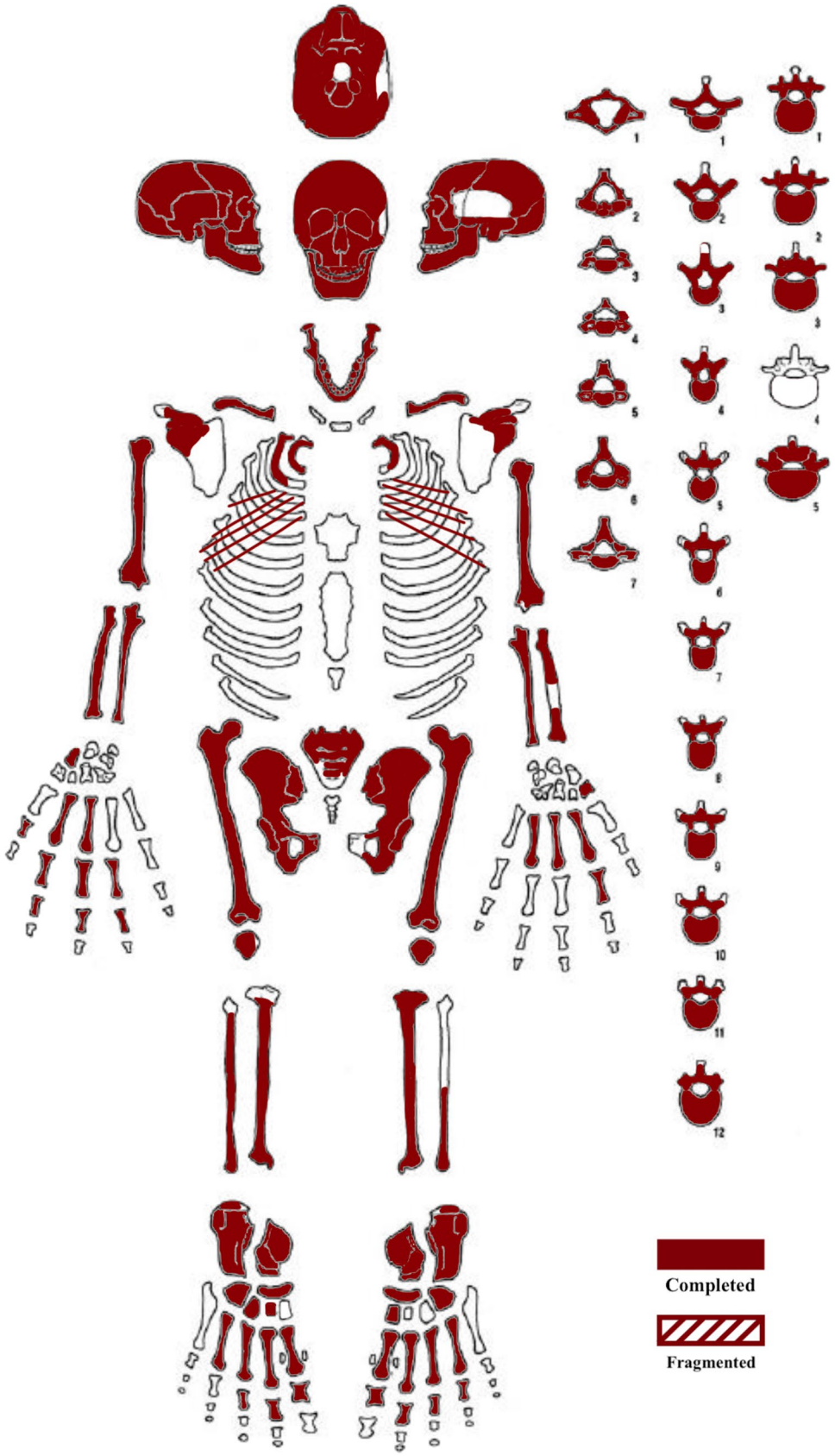

Fig. 5 State of preservation of the skeleton found in *Burial 2*. Complete bones are fully coloured in red, while the fragmented ones (e.g. ribs) are indicated by means of red oblique lines

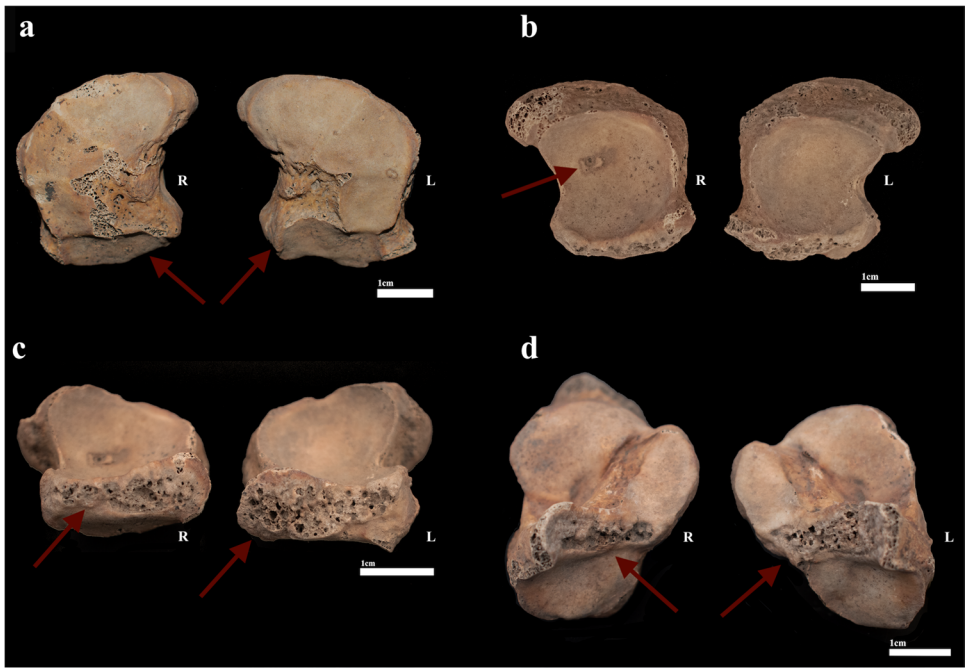

Fig. 6 Anterior (**a**) and posterior (**b**) views of the navicular bones: **a** the arrows indicate the enlarged size of the naviculars caused by their fusion with a portion of the anterior facet of the calcaneus; **b** the arrow indicates the likely osteochondritis dissecans on the right navicular bone. **c**, **d**: views of the matching lesions with their roughened aspect (arrows)

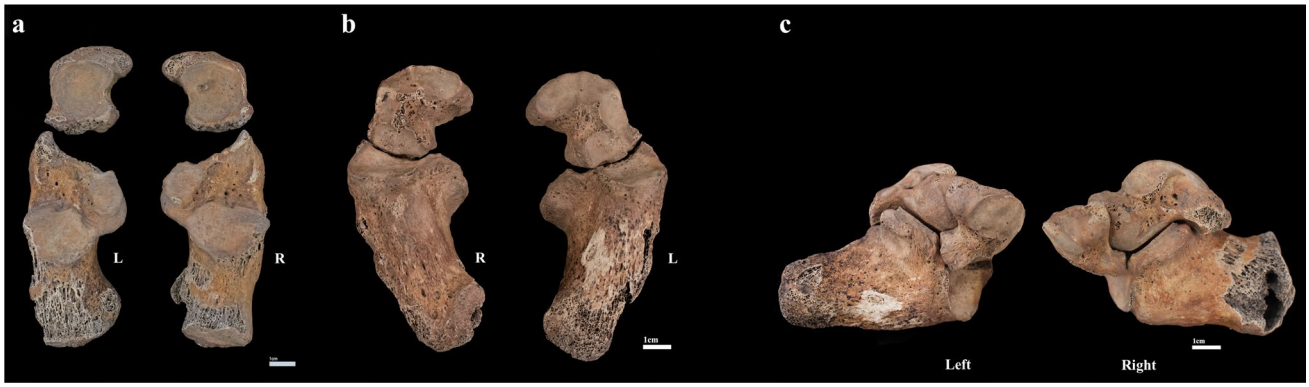

Fig. 7 Superior (**a**) and inferior (**b**) views of left and right calcanei and navicular bones. Lateral (**c**) view of articulated calcanei, tali, and navicular bones of the feet

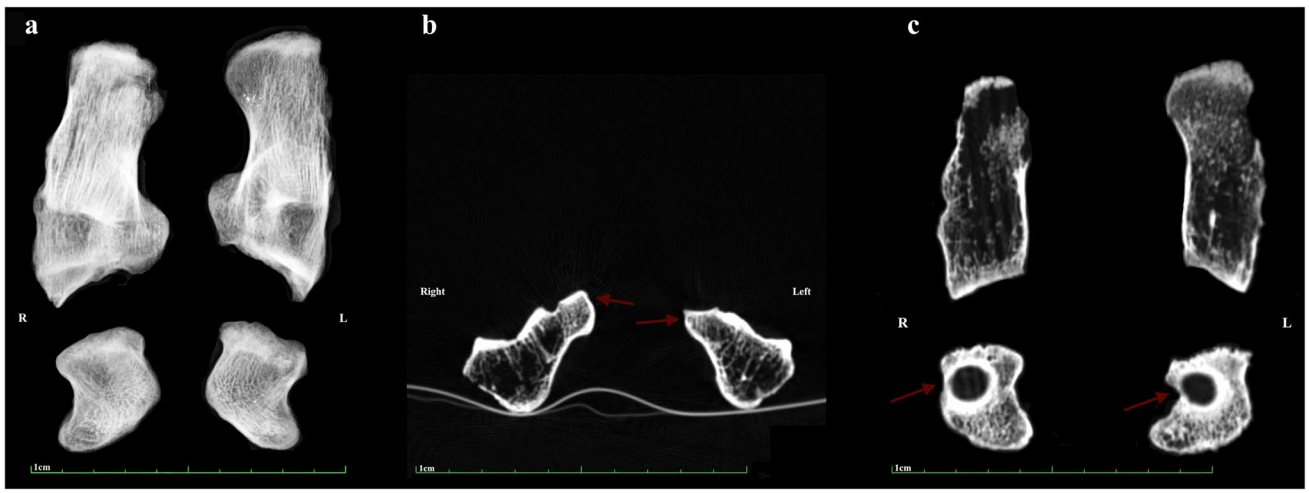

Fig. 8 Antero-posterior X-ray image (**a**) of the calcanei and navicular bones, coronal CT scan (**b**) of the anterior talar facet (the arrows show the *sustentaculum tali*), and transverse CT scan (**c**) of the calcanei and navicular bones with circular lack of bone tissue (arrows)

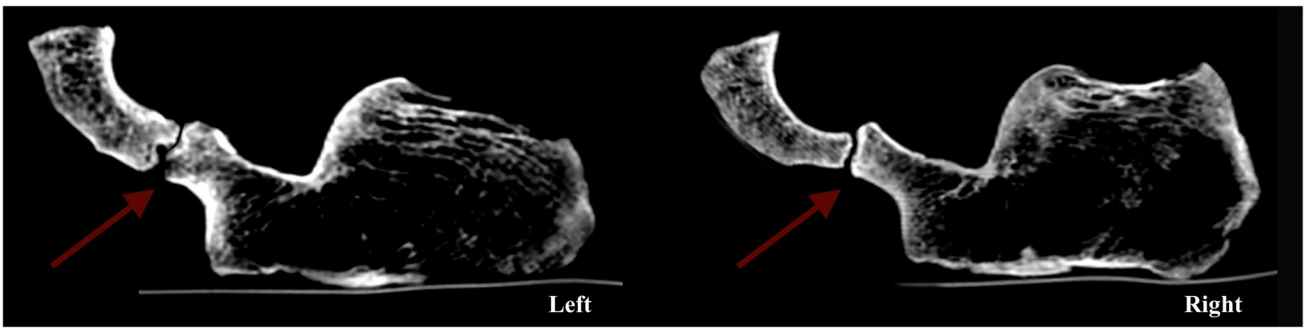

Fig. 9 Sagittal CT scan view of the two calcanei and navicular bones with the 'anteater nose sign' (arrows)

Considering differential diagnoses, the following ones can be evaluated: infection, trauma, degenerative joint disease (osteoarthritis), and osteochondritis dissecans. The first three possibilities can be excluded on the basis of the lack of traces of infectious diseases or traumatic events, nor could evident signs of age and work-related chronic arthritis be detected. Osteochondritis dissecans also sharply differs from tarsal coalition in its morphology, since it has a strong necrotic component (Vikatou et al. 2017). However, it can be suspected that this disease is indeed present in the right navicular on its concave articular surface (Fig. 6b).

These considerations lead to the sole possible conclusion that the presented case is a non-osseous instance of tarsal coalition and, additionally, to the fact that it belongs to the congenital type. This is corroborated by evidence that the studied individual's skeleton does not show any traces of diseases typically leading to fusion of two bones nor bony calluses, as well as no fracture lines be detected through the radiological examination, to which it can supplemented that the individual's foot anatomy appears to represent a functional unit.

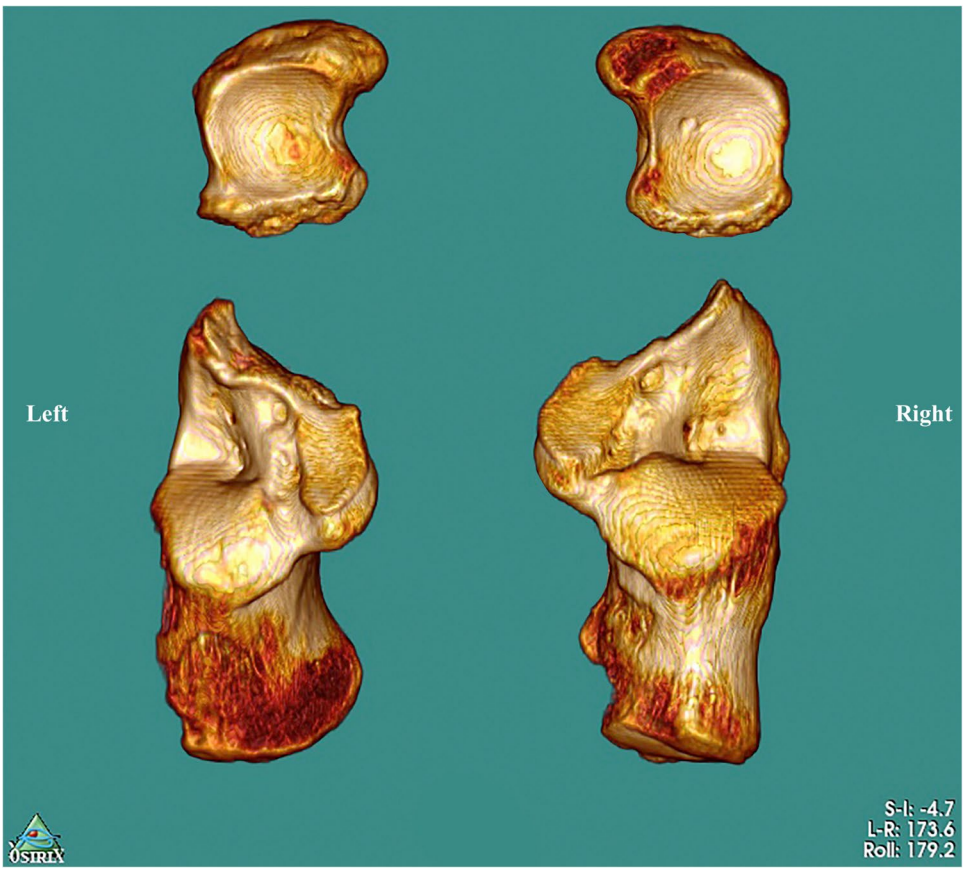

Fig. 10. 3D virtual reconstruction of the bilateral non-osseous calcaneonavicular coalition

From the clinical perspective, calcaneonavicular coalition can either present symptomatically or asymptomatically, which cannot be ultimately ascertained although the abnormal angulation (outward rotation) of the podal bones may well have resulted in postural and deambulation issues with subsequent biomechanical stress and likely painful manifestations. Among the most usually described symptoms in the modern clinical setting, limitation of subtalar and midtarsal joint motion, foot arch pain, and rigid peroneal spastic flat foot are to be considered (Kulik and Clanton 1996), and future biomechanical analyses may add more specific data.

Conclusions

In this study, we focus on the analysis of bone remains with the combined use of photogrammetric and stereophotogrammetric elaborations of multiple photographic acquisitions realised during the archaeological excavation, radiocarbon dating, and ending with a comprehensive palaeopathological study. To the best of our knowledge, the mediaeval adult female of *Burial 2* represents the earliest known case of bilateral non-osseous calcaneonavicular coalition in the Italian anthropological record. Future analyses will be conducted in order to determine whether other conditions, for instance genetic syndromes, were present in this individual. Finally, due to the fact that this congenital condition, as proved by Leonard (1974), has a strong inheritance component, the continued excavation and study of the Troina necropolis will help us understand the actual prevalence of CN coalition and familial links in this mediaeval Sicilian population.

Acknowledgements We wish to thank Salvatore Gueli (former Superintendent of Enna, Department of Cultural and Environmental Heritage), Pinella Marchese, Giovanna Susan (former Director of the *Polo Regionale di Piazza Armerina*), and Rosario Patanè who gave us the authorisation to conduct our studies. Special thanks go to the Mayor of Troina, Sebastiano Fabio Venezia, and his staff for their — not only financial — support during our stay in Troina. Last but not least, we would like to mention the particular dedication shown during the excavation by the students from the 'ArcheoTroina' project (University of Messina), in particular Elisa Misiano, Anna Romeo, and Clelia Marchese. We also wish to thank Nunzio di Bartolo (MD) and Lidia Zietek (Casa di Cura 'Santa Lucia', Siracusa, Sicily) for their help with the radiological analysis and Carmine Lubritto (The University of Campania 'Luigi Vanvitelli') for the ^{14}C data.

Funding This work was financially supported by the Municipality of Troina (Enna).

Declarations

Conflict of interest The authors declare no competing interests.

References

Agochukwu NB, Solomon BD, Benson LJ, Muenke M (2013) Talocalcaneal coalition in Muenke syndrome: report of a patient, review of the literature in FGFR-related craniosynostoses, and consideration of mechanism. Am J Med Genet A 161A(3):453–460

Albee ME (2020) Diagnosing tarsal coalition in mediaeval Exeter. Int J Paleopathol 28:32–41

Angel JL (1971) The people of Lerna: analysis of a prehistoric Aegean population. Smithsonian Institution Press, Washington, DC; p 55, plate XIV (fig. 122)

Aufderheide AC, Rodríguez-Martín C (2011) The Cambridge encyclopedia of human paleopathology. Cambridge University Press, , Cambridge, p 75

Bello S (2001) Tafonomia dei resti ossei umani. Effetti dei processi di conservazione dello scheletro sui parametri antropologici. Tesi di dottorato in Antropologia. Università degli studi di Firenze – Université de la Mediterranée de Aix-Marseille, Faculté de Medicine

Bohne WH (2001) Tarsal coalition. Curr Opin Pediatr 13(1):29–35

Brooks S, Suchey JMS (1990) Skeletal age determination based on the os pubis: a comparison of the Acsádi-Nemeskéri and Suchey-Brooks methods. Hum Evol 5:227–238

Carandini A (2010) Storie dalla terra. Manuale di scavo archeologico. Einaudi, Torino

Case D, Burnett S (2012) Identification of tarsal coalition and frequency estimates from skeletal samples. Int J Osteoarchaeol 22:667–684

Case DT (2014) Bones of the hands and feet. In: Owsley DW, Richard LJ (eds) Kennewick Man: The Scientific Investigation of an Ancient American Skeleton. Texas A&M Press, College Station

Craig CL, Goldberg MJ (1977) Calcaneocuboid coalition in Crouzon's syndrome (craniofacial dysostosis): report of a case and review of the literature. J Bone Jt Surg 59(6):826–827

Darton Y (2007) Flatfoot: the paleopathological diagnosis. Int J Osteoarchaeol 17:286–298

Dastugue J, Metz F (1977) Bloc calcanéo-naviculaire bilatéral sur un squelette mérovingien. J Med Caen 12:137–140

Dinwiddy KE (2009) A late Roman cemetery at Little Keep, Dorchester, Dorset. Wessex Archaeology, Salisbury

Dixon M, Armstrong P, Stevens D et al (2001) Identical mutations in NOG can cause either tarsal/carpal coalition syndrome or proximal symphalangism. Genet Med 3:349–353

Docquier PL, Maldaque P, Bouchard M (2019) Tarsal coalition in paediatric patients. Orthop Traumatol Surg Res 105(1S):S123–S131

Ferembach D, Schwidetzky I, Stloukal M (1977–1979) Raccomandazioni per la determinazione dell'età e del sesso sullo scheletro. Rivista di Antropologia 60:5–51

Fiorini A, Archetti V (2011) Fotomodellazione e stereofotogrammetria per la creazione di modelli stratigrafici in archeologia dell'architettura. Archeologia e Calcolatori 22:199–216

Harris RI (1965) Retrospect-peroneal spastic flat foot (rigid valgus foot). Follow-up notes on articles previously published in the journal. J Bone Jt Surgery 47A:1657–1667

Harris RI (1955) Rigid valgus foot due to talocalcaneal bridge. J Bone Jt Surgery 37A:169–183

Heiple KG, Lovejoy CO (1969) The antiquity of tarsal coalition. Bilateral deformity in a pre-Columbian Indian skeleton. J Bone Jt Surgery 51(5):979–983

Hynes RA, Romash MM (1987) Bilateral symmetrical synchondrosis of navicular first cuneiform joint presenting as a lytic lesion. Foot Ankle Int 8(3):164–168

Jaff M (2005) Rilievo fotogrammetrico dell'architettura. Alinea, Firenze

Kulik SA Jr, Clanton TO (1996) Tarsal coalition. Foot Ankle Int 17(5):286–296

Leonard MA (1974) The inheritance of tarsal coalition and its relationship to spastic flat foot. J Bone Jt Surgery 56B:520–526
Lovejoy CO, Meindl RS, Pryzbeck TR, Mensforth RP (1985) Chronological metamorphosis of the auricular surface of the ilium: a new method for determination of adult skeletal age at death. Am J Phys Anthropol 68:15–28
Lovejoy CO (1985) Dental wear in the Libben population: its functional pattern and role in the determination of adult skeletal age at death. Am J Phys Anthropol 68:47–56
Militello E (1961) Troina. Scavi effettuati dall'Istituto di archeologia dell'Università di Catania negli anni 1958 e 1960. Notizie Degli Scavi Di Antichità 15:322–404
Oestreich AE, Mize WA, Crawford AH, Morgan RC Jr (1987) The "anteater nose": a direct sign of calcaneonavicular coalition on the lateral radiograph. J Pediatr Orthop 7:709–711
Pfitzner W (1896) Beiträge zur Kenntnis des Menschlichen Extremitätenskelets: VII. Die Variationen in Aufbau des Fusskelets. In: Schwalbe G (ed) Morphologische Arbeiten. Gustav Fischer, Jena, pp. 245–527
Phenice TW (1969) A newly developed visual method of sexing the os pubis. Am J Phys Anthropol 30:297–301
Rühli FJ, Solomon LB, Henneberg M (2003) High prevalence of tarsal coalitions and tarsal joint variants in a recent cadaver sample and its possible significance. Clin Anat 16(5):411–415
Scibona G (1980) Troina I: 1974–1977. Nuovi dati sulla fortificazione ellenistica e la topografia del centro antica. Archivio Storico Messinese 31:348–389
Silva AM (2005) Non-osseous calcaneonavicular coalition in the Portuguese prehistoric population: report of two cases. Int J Osteoarchaeol 15:449–453
Silva AM (2011) Foot anomalies in the Late Neolithic/Chalcolithic population exhumed from the rock cut cave of São Paulo 2 (Almada, Portugal). Int J Osteoarchaeol 21:420–427
Silva AM, Silva AL (2010) Unilateral non-osseous calcaneonavicular coalition: report of a Portuguese archeological case. Anthropol Sci 118(1):61–64
Stormont DM, Peterson HA (1983) The relative incidence of tarsal coalition. Clin Orthop Relat Res 181:28–36
Swensen SJ, Otsuka NY (2015) Tarsal coalitions–calcaneonavicular coalitions. Foot Ankle Clin 20(4):669–679
Trotter M, Gleser GC (1952) Estimation of stature from long bones of American Whites and Negroes. Am J Phys Anthropol 10:463–514
Trotter M, Gleser GC (1977) Corrigenda to estimation of stature from long limb bones of American Whites and Negroes. Am J Phys Anthropol 47:355–356
Vargová L, Horáčková L, Horáková M, Eliášová H, Myšková E, Ditrich O (2016) Paleopathological, trichological and paleoparasitological analysis of human skeletal remains from the migration period cemetery Prague-Zličín. IANSA 7(1):13–32
Varotto E, Militello PM, Platania E, Sferrazza P, Galassi FM (2021) Paleopathological study of a podal osteochondroma from the prehistoric Hypogeum of Calaforno (Sicily). Clin Anat 34(1):19–23
Vikatou I, Hoogland MLP, Waters-Rist AL (2017) Osteochondritis dissecans of skeletal elements of the foot in a 19th century rural farming community from the Netherlands. Int J Paleopathol 19:53–63